Zhang et al. *Zool. Res.* 2022, 43(3): 331−342
https://doi.org/10.24272/j.issn.2095-8137.2022.045

ZR | Zoological Research

Article Open Access

Phylogenetic relationships of the zokor genus *Eospalax* (Mammalia, Rodentia, Spalacidae) inferred from whole-genome analyses, with description of a new species endemic to Hengduan Mountains

Tao Zhang[1], Meng-Long Lei[1], Hao Zhou[2,3], Zhong-Zheng Chen[1,4,*], Peng Shi[1,5,6,*]

[1] *State Key Laboratory of Genetic Resources and Evolution*, *Kunming Institute of Zoology*, *Chinese Academy of Sciences*, *Kunming*, *Yunnan* 650204, *China*

[2] *Jiangsu Key Laboratory of Neuropsychiatric Diseases and College of Pharmaceutical Sciences*, *Soochow University*, *Suzhou*, *Jiangsu* 215123, *China*

[3] *Joint Laboratory of Animal Models for Human Diseases and Drug Development*, *Soochow University and Kunming Institute of Zoology*, *Chinese Academy of Sciences*, *Kunming*, *Yunnan* 650223, *China*

[4] *Collaborative Innovation Center of Recovery and Reconstruction of Degraded Ecosystem in Wanjiang Basin Co-founded by Anhui Province and Ministry of Education*, *School of Ecology and Environment*, *Anhui Normal University*, *Wuhu*, *Anhui* 241000, *China*

[5] *School of Future Technology*, *University of Chinese Academy of Sciences*, *Beijing* 100049, *China*

[6] *Center for Excellence in Animal Evolution and Genetics*, *Chinese Academy of Sciences*, *Kunming*, *Yunnan* 650223, *China*

ABSTRACT

Zokors in the genus *Eospalax*, which are endemic to northern and western China, are subterranean rodents that inhabit various niches, including grasslands, high-altitude meadows, forests, and farmlands. Six species in *Eospalax* were described a century ago but their taxonomy and phylogeny remain controversial. In this study, we performed high-depth whole-genome sequencing of 47 zokor samples, comprising all six previously described species. Genomic analyses revealed a reliable and robust phylogeny of *Eospalax* and supported the validity of the six named species. According to the inferred phylogenetic relationships, *Eospalax* first divergent into two clades in the early Pliocene (ca. 4.68 million years ago (Ma)), one inhabiting the high-altitude Qinghai-Xizang (Tibet) Plateau (QTP) and adjacent regions, and the another inhabiting the low-altitude Loess Plateau and Qinling-Daba Mountains. The most recent divergences occurred between *E. baileyi* and *E. smithii* and between *E. rufescens* and *E. rothschildi* in the late Pliocene (ca. 2.09 and 2.19 Ma, respectively). We also collected specimens of zokors in the southern Hengduan Mountains (Muli County, Sichuan Province), far from the known distributions of all other zokors. Morphological and

Received: 21 February 2022; Accepted: 17 March 2022; Online: 17 March 2022

Foundation items: This study was supported by the Second Tibetan Plateau Scientific Expedition and Research (STEP) Program (2019QZKK05010218, 2019QZKK05010110), National Natural Science Foundation of China (32100339, 31871277). P.S. was supported by the Yunling Scholar Project, Ten-Thousand Talents Plan of Yunnan Province. T.Z. was supported by the Youth Innovation Promotion Association, Chinese Academy of Sciences

*Corresponding authors, E-mail: zhongzheng112@126.com; ship@mail.kiz.ac.cn

molecular analyses strongly suggested that the specimens represent a new species, formally described here as *Eospalax muliensis* **sp. nov**. The new species belongs to the high-altitude clade and diverged from closely related species (ca. 4.22 Ma) shortly after the first divergence in *Eospalax*. Interestingly, *Eospalax muliensis* **sp. nov**. possesses more supposedly plesiomorphic characters, suggesting a possible origin of the genus in the Hengduan Mountains.

Keywords: Zokor; *Eospalax*; Phylogenomic analyses; New species; Hengduan Mountains

INTRODUCTION

Zokors (subfamily Myospalacinae) are a group of strictly subterranean rodents endemic to East Asia, which belong to the family Spalacidae and are closely related to the Rhizomyinae and Spalacinae subfamilies (Bouckaert et al., 2019; Guo et al., 2021; Lin et al., 2014; Norris et al., 2004). Zokors are cylindrical in shape, with stocky and strong forelimbs and hardened nose pads to excavate their complex burrow systems. Based on morphological and molecular evidence, extant zokors are classified into two genera: i.e., *Myospalax*, which includes species with flat occiputs, and *Eospalax*, which includes species with convex occiputs (Su et al., 2014; Zheng, 1994; Zhou & Zhou, 2008). *Myospalax* species are mainly distributed in the grasslands of northeast China, Mongolia, and Russia, while *Eospalax* species inhabit various niches in northern and western China (Figure 1A) (Fan & Shi, 1982), including the high-altitude Qinghai-Xizang (Tibet) Plateau (QTP). The phenotypic and genetic adaptations of the plateau zokor (*E. baileyi*) to the hypoxic conditions on the QTP have been well researched (Wei et al., 2006; Xu et al., 2021; Zhang et al., 2021).

However, despite studies on the physiology, ecology, and genetics of certain species, the taxonomy and phylogeny of *Eospalax* remain controversial. Six species of *Eospalax* were described in the late 19th and early 20th century, but the taxonomic status of *Eospalax* species has changed with time, especially for *E. baileyi*, *E. cansus*, and *E. rufescens* (Table 1). *Eospalax fontanierii*, *E. rothschildi*, and *E. smithii* were recognized as distinct species by Allen (1940), with this classification adopted by many monographs until recently (Smith & Xie, 2008; Wilson & Reeder, 2005). Based on comprehensive morphological comparisons, Fan & Shi (1982) found that *E. cansus* is stably smaller than *E. fontanierii* in body size and skull and *E. baileyi* is distinct from *E. fontanierii* in nose pad shape and presence of a postero-external lobe on M^3. Thus, they elevated *E. baileyi* and *E. cansus* to species level. Subsequent studies using mitochondrial DNA markers have generally validated the status of all six *Eospalax* species (He et al., 2012; Su et al., 2014; Zhou & Zhou, 2008). However, the classification of *E. baileyi* has remained somewhat controversial due to insufficient molecular markers and incomplete sampling (Jiang et al., 2017; Wei et al., 2021). In addition, the potential existence of new undescribed species within the *Eospalax* genus may complicate established taxonomy. Here, based on a literature review of species distribution, we found reports of zokors in the southern Hengduan Mountains (Muli County, Sichuan

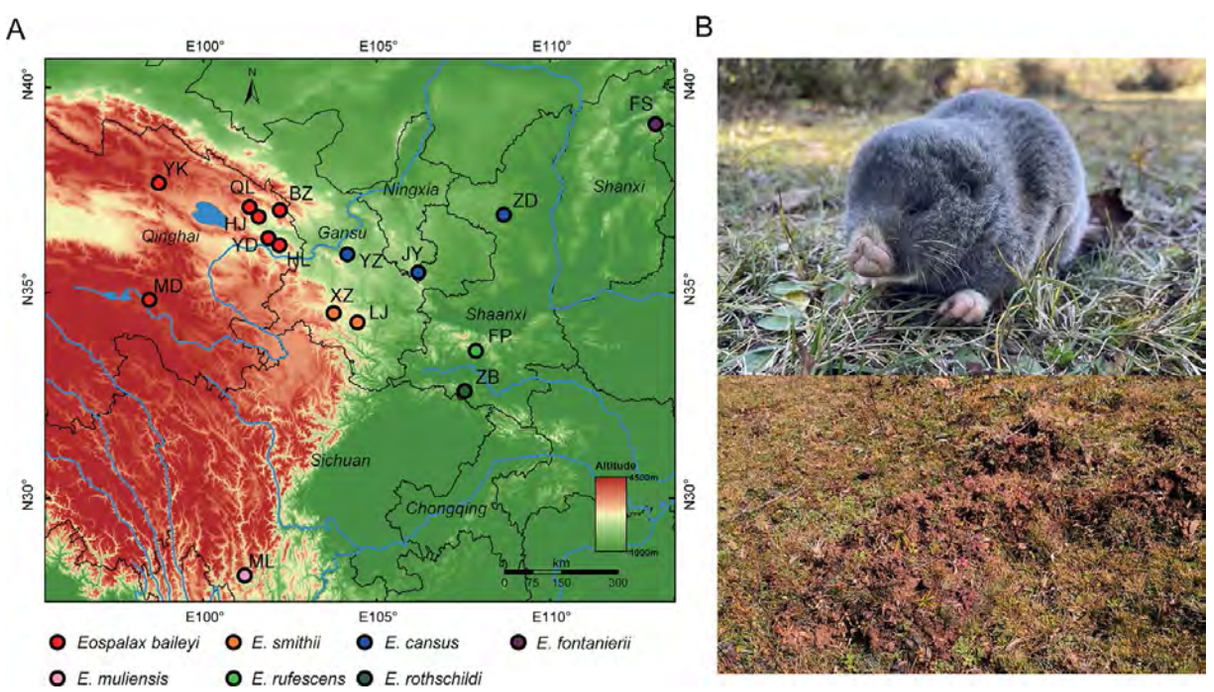

Figure 1 Sampling of species in *Eospalax*

A: Geographic distribution of sampling sites. B: Image of typical *Eospalax muliensis* **sp. nov.** (upper panel) and aboveground mound (lower panel). Photo by Hao Zhou.

Table 1 Previous and proposed classifications of *Eospalax* genus

Allen (1940)	Fan & Shi (1982)	Song (1986)	Li & Chen (1989)	Jiang et al (2017)	Wei et al (2021)	Present study
fontanierii	*fontanierii*	*fontanierii*	*fontanierii*	*fontanierii*	*fontanierii*	*fontanierii*
(fontanierii)	*cansus*	*cansus*	*(fontanierii)*	*rothschildi*	*cansus*	*cansus*
(cansus)	*(cansus)*	*rothschildi*	*(baileyi)*	*rufescens*	*baileyi*	*baileyi*
(baileyi)	*(rufescens)*	*rufescens*	*(cansus)*	*smithii*	*rothschildi*	*smithii*
rothschildi	*rothschildi*	*(rufescens)*	*(rufescens)*	*cansus*	*rufescens*	*rothschildi*
smithii	*smithii*	*(baileyi)*	*rothschildi*		*smithii*	*(rothschildi*)*
	baileyi		*(rothschildi)*			*(hubeiensis*)*
			(hubeiensis)			*rufescens*
			smithii			*muliensis*

Recognized species (subspecies) are presented, but not synonyms. *: These two subspecies were not verified in present study but followed Li & Chen (1989).

Province) (Liu et al., 2007), far from the known distribution of all other zokors (Figure 1A). Thus, in the current study, we collected 14 *Eospalax* specimens from Muli County between October 2020 and October 2021. Externally, these zokors differed considerably from all other known species due to their small size and long tail (Figure 1B), indicating that they may represent a distinct taxon, which we name herein as *Eospalax muliensis* **sp. nov**.

In addition to taxonomic controversies, the phylogeny of *Eospalax* remains incomplete and inconsistent. Conflicting phylogenies among *Eospalax* species have been reported in previous studies based on both mitochondrial DNA markers (Cai et al., 2020; Su et al., 2014; Zhou & Zhou, 2008; Zou et al., 2020) and morphological traits (Li & Chen, 1986; Li & Wang, 1996). Notably, phylogenetic relationships inferred from mitochondrial markers are unstable when different markers or tree-construction methods are applied (Su et al., 2014; Zhou & Zhou, 2008). Therefore, the ambiguous and conflicting phylogenetic relationships reported in *Eospalax* hamper studies of this remarkable lineage and underscore the need for a reliable and robust phylogeny.

In the current study, we aimed to clarify the taxonomy and phylogeny of *Eospalax*. All six known species of *Eospalax* were sampled and whole genomes were sequenced to high depth. Whole-genome analysis revealed reliable and robust phylogenetic relationships and validated the status of all six previously described species. Furthermore, by integrating morphological and genomic evidence, the zokor specimens collected from Muli County were found to represent a new species. Thus, the phylogeny and diversification of the new species were also studied.

MATERIALS AND METHODS

Sample collection

Fieldwork was carried out from April 2017 to October 2021. Skeletal muscle was collected for DNA extraction. All collections followed the animal use protocols approved by the Animal Care and Ethics Committee of the Kunming Institute of Zoology (KIZ), Chinese Academy of Sciences (CAS) (Approval No. SMKX-SQ-2021-067).

Sampling sites of each species were located in their generally acknowledged distribution areas (Figure 1A; Supplementary Table S1). The seven sampling sites of *E. baileyi* were reported in our previous work (Zhang et al., 2021). Because the distribution of *E. cansus* is wide and adjacent to several other species in *Eospalax*, three sampling sites of *E. cansus* were chosen across Shaanxi, Ningxia, and Gansu provinces to ensure representativeness. For other species, one or two sampling sites were selected. Two zokors collected near Hulun Lake (Inner Mongolia Autonomous Region, China) were recognized as *Myospalax psilurus* according to their skull and hairless tails. Thus, these two zokors were used as an outgroup.

Whole-genome sequencing and *de novo* assembly-based variant calling

In this study, 47 zokor samples were collected and whole genomes were sequenced to a high depth, with an average of 137.2 Gb of data for each sample (Figure 1A; Supplementary Table S1). Combined with previously reported whole-genome sequences of 38 *E. baileyi* samples (Zhang et al., 2021), our dataset covered all six previously described *Eospalax* species, as well as *Eospalax muliensis* **sp. nov**. and two samples of closely related *M. psilurus*.

DNA extraction, resequencing library construction, and quality control of raw sequencing reads were performed following Zhang et al (2021). Briefly, the resequencing library was constructed following standard protocols and sequenced using Illumina HiSeq or BGISEQ paired-end mode. Raw sequencing reads were trimmed using Trimmomatic v0.36 (Bolger et al., 2014) to remove low-quality reads. Although a *E. baileyi* genome assembly was recently published (Zhang et al., 2021), all other zokor genomes are currently unavailable. Thus, we sequenced all samples to high depth and applied *de novo* assembly-based variant calling following the FermiKit pipeline (Li, 2015b). For comparability, variant calling of all *E. baileyi* samples was also applied using this pipeline. First, clean reads of each sample were error corrected using BFC v.r181 (Li, 2015a). Second, Fermi2 v.r178 (Li, 2012) was used to *de novo* assemble the genome of each sample. Third, the assembly of each sample was mapped to the plateau zokor genome using minimap2 v.2.17 (Li, 2018) with parameters "-ax asm5/asm10/asm20 -k 23 -w 11 -f 1000 -n 2 -s 100 --end-bonus 5". According to the genetic distance between samples and plateau zokors, different parameters of -ax were applied to balance the sensitivity and specificity of mapping. Specifically, asm5, asm10, and asm20 were applied for

samples of *E. baileyi*, *E. smithii*, and all other species, respectively. After mapping, all sample variants were called jointly using the "pileup" functions in HTSbox v.r310 with parameters " -d -V 0.15 -S 300 -q 20 -Q 3 -s 5". Raw genotypes were first filtered according to allele balance. For homozygous genotypes, at least 90% of reads should support these genotypes. For heterozygous genotypes, the two types of alleles should have 25%–75% of read-support simultaneously. If the above criteria were not satisfied, the genotypes were set as missing. After allelic balance filtering, we only retained those biallelic single nucleotide variants (SNVs) with a missing rate of no more than 20% using VCFtools v.0.1.17 (Danecek et al., 2011).

Phylogenomic analyses

Phylogenetic relationships among all zokor samples were inferred using whole-genome SNVs and maximum-likelihood (ML) algorithms. Considering the computational resources required, we pruned high-quality SNVs by randomly choosing one SNV in each 100 bp window across the genome. ML analyses were conducted in RAxML v.8.2.12 (Stamatakis, 2014) with the nucleotide substitution model of GTRGAMMA. To test the reliability of inferred phylogenetic relationships, 100 bootstraps were applied.

In addition to the construction of phylogenetic trees based on whole-genome pruned SNVs, we also applied a summary of sliding-window ML trees. First, we split the whole genomes into over 50 000 non-overlapping windows (each 50 kb long). For each window, ML trees were constructed using RAxML based on all high-quality SNVs. Weighting and summary of all sliding-window ML trees across whole genomes were explored using topology weighting by iterative sampling of subtrees (Twisst) (Martin & van Belleghem, 2017).

Divergence time among all species in the genus *Eospalax* was determined using SNAPP v2.6.2 (Bryant et al., 2012) in BEAST2 (Bouckaert et al., 2019). Secondary calibration was applied following He et al (2020), which estimated that the divergence between *Myospalax* and *Eospalax* occurred 8.8 million years ago (Ma), with a 95% highest posterior density (HPD) interval from 7.43 to 10.23 Ma. The estimate from He et al (2020) is congruent with fossil records of the genus *Myotalpavus*, which occurred in the Late Miocene and may be the ancestor of both *Eospalax* and *Myospalax* (Zheng, 1994). Thus, we constrained the divergence time between *Myospalax* and *Eospalax* with a lognormal distribution centered at 8.8 Ma and a standard deviation of 0.085 in SNAPP analysis. For each species, the individual with the lowest proportion of missing data was used to represent that species. The SNVs were first pruned as described previously, with those identified as monomorphic or containing missing data then filtered. Finally, 100 000 randomly selected SNVs were used, and 10 million Markov Chain Monte Carlo (MCMC) iterations were set for SNAPP analysis. Convergence was assessed using Tracer v1.6 (Rambaut et al., 2018) with 10% burn-in. DensiTree v.2.6.2 (https://www.cs.auckland.ac.nz/~remco/DensiTree/) was used to visualize all posterior trees sampled by SNAPP. TreeAnnotator v2.6.2 (https://beast.community/treeannotator) was used to quantify the posterior probabilities of clades as node support in a maximum clade credibility tree with 10% burn-in. Divergence time and phylogenetic relationships were visualized in FigTree v1.4.4 (http://tree.bio.ed.ac.uk/software/figtree/). SNAPP analysis was implemented three times independently and obtained nearly identical results.

Absolute genetic distance (D_{XY}) among species was estimated in 50 kb windows with a 50 kb step size along the genome using popgenWindows.py in genomics_general (https://github.com/simonhmartin/genomics_general). We excluded windows located in scaffolds <1 Mb due to possible poor assembly of short scaffolds.

Mitochondrial genome (mitogenome) analysis

For all whole-genome sequenced samples, we assembled their mitogenomes. We randomly selected 5 Gb of resequencing reads for each sample. Assembly was performed using MitoZ v.2.3 (Meng et al., 2019) or GetOrganelle v.1.7.2b (Jin et al., 2020) with default parameters. The mitogenome of a published *M. psilurus* sample (JX014234) (Li et al., 2016) served as a reference in GetOrganelle analysis. Annotation of the assembled mitogenomes was performed with MitoZ. The quality of each mitogenome was carefully checked based on length (>16 kb), gene count (37 genes), and circularity.

In addition to the mitogenomes assembled in this study, we downloaded all other mitogenomes in *Eospalax* and *Myospalax* reported in previous studies. Thirteen protein-coding genes and two ribosomal RNA (rRNA) genes were included in the following analyses. Gene alignments were performed by CLUSTAL v.2.1 (Larkin et al., 2007) and then concatenated. The best partition schemes for the dataset were identified using PartitionFinder v.2.1.1 (Lanfear et al., 2017) with recommended corrected Akaike Information Criterion (AICc). This analysis partitioned 15 mitochondrial genes into eight subsets. Mitochondrial phylogenomic analyses were inferred using RAxML with 1 000 bootstrap replicates.

Morphological data and analyses

A total of 62 specimens of *Eospalax* were collected. All specimens and tissue samples were deposited in KIZ, CAS. Specimens were identified following Fan & Shi (1982) and Luo et al (2000). Forty-eight specimens were assigned to the six recognized species, including *E. baileyi* (*n*=34), *E. cansus* (*n*=5), *E. fontanierii* (*n*=1), *E. rothschildi* (*n*=2), *E. rufescens* (*n*=2), and *E. smithii* (*n*=4). Fourteen specimens collected from Muli County, Sichuan Province, were assigned to the putative new species (*Eospalax muliensis* **sp. nov.**).

The body weight (BW) of each specimen was weighed up to 0.01 g using an electronic scale. External measurements, including head and body length (HB), tail length (TL), and hindfoot length (HF), of some individuals were taken in the field using a ruler to the nearest 0.1 mm. Twenty-one cranial and dental measurements were taken using a digital caliper graduated to 0.01 mm following Pan et al (2007). These measurements included greatest length of skull (GLS), condylobasal length (CBL), basal length (BL), palatal length (PL), zygomatic width (ZMW), interorbital breadth (IOB), foramen infraorbital breadth (FIB), rostrum width (RSW), mastoid width (MTW), maximum width across upper second molars (M^2–M^2), length of upper tooth row (LUTR), length of upper molars (LUM), nasal length (NSL), braincase height

(BCH), greatest breadth of foramen magnum (GBFM), length of auditory bulla (LAB), distance between auditory bulla (DAB), mandibular length (MDL), length of below toothrow (LBTR), length of lower molars (LLM), and length of lower incisor (LLI). We performed principal component analysis (PCA) to analyze morphometric variation of these specimens in SPSS v19.0 (SPSS Inc., USA). PCA was only based on the 21 craniodental measurements of adult specimens. All craniodental variables were $\log_{10}$-transformed before PCA. We considered any component with an eigenvalue exceeding 1.0 to be meaningfully interpretable. We further examined specimen morphology as per Fan & Shi (1982), Song (1986), and Luo et al (2000), and followed their terminologies for morphological descriptions.

RESULTS

Phylogenetic relationship and molecular dating

A total of 85 whole-genome sequenced samples were included in this study (Figure 1A; Supplementary Table S1), covering all six previously described *Eospalax* species as well as *Eospalax muliensis* **sp. nov.** and two samples of closely related *Myospalax psilurus*.

After stringent quality control of genome alignment and variant calling, ~227 million high-quality SNVs were identified. Based on the genome-wide SNVs, ML analysis yielded a highly resolved phylogeny. All nodes that separated species within the genus *Eospalax* exhibited 100% bootstrap support (Figure 2A). Accordingly, species in *Eospalax* could be divided into two major clades (i.e., high- and low-altitude clades). The high-altitude clade, comprised of *E. baileyi*, *E. smithii*, and *Eospalax muliensis* **sp. nov**., generally inhabited the high-altitude QTP and adjacent regions (2 700–4 300 m a.s.l.), while the low-altitude clade, comprised of the other four *Eospalax* species, generally inhabited the relatively low-altitude Loess Plateau and Qinling-Daba Mountains. Within the high-altitude clade, *Eospalax muliensis* **sp. nov**. was found in a basal position and inhabited extremely high altitudes (3 700 m a.s.l.). Within the second clade, *E. fontanierii* split first from the other species. Notably, three *E. cansus* populations located remotely from each other formed a tight monophyletic cluster.

The genetic distances between the *M. psilurus* outgroup and species in *Eospalax* ranged from 3.5% to 3.7% (Figure 2B). Within the genus *Eospalax*, the genetic distances among species ranged from 1.0% to 2.2% (Figure 2B). For each species pair separated by the same internal node, their genetic distances were comparable (Figure 2B), demonstrating the reliability of the inferred phylogenetic relationships and that the applied methods enabled phylogenomic analysis.

Phylogenetic relationships inferred from the mitogenomes were also constructed (Supplementary Figure S1). Consistent with nuclear genomic analyses, *Eospalax muliensis* **sp. nov**. was also identified as a distinct genetic lineage based on mitogenomic analyses (Supplementary Figure S1). However, significant incongruences among phylogenies inferred from nuclear genomes and mitogenomes were found, especially in the positions of *Eospalax muliensis* **sp. nov**. and *E. fontanierii* (Figure 2A; Supplementary Figure S1) (see Discussion).

To confirm the inferred phylogenetic relationships and investigate the alternative topology, we split the genomes into >50 000 windows (50 kb in size) and constructed window trees based on the corresponding SNVs in each window. Most window trees (75.8%) were consistent with the whole-

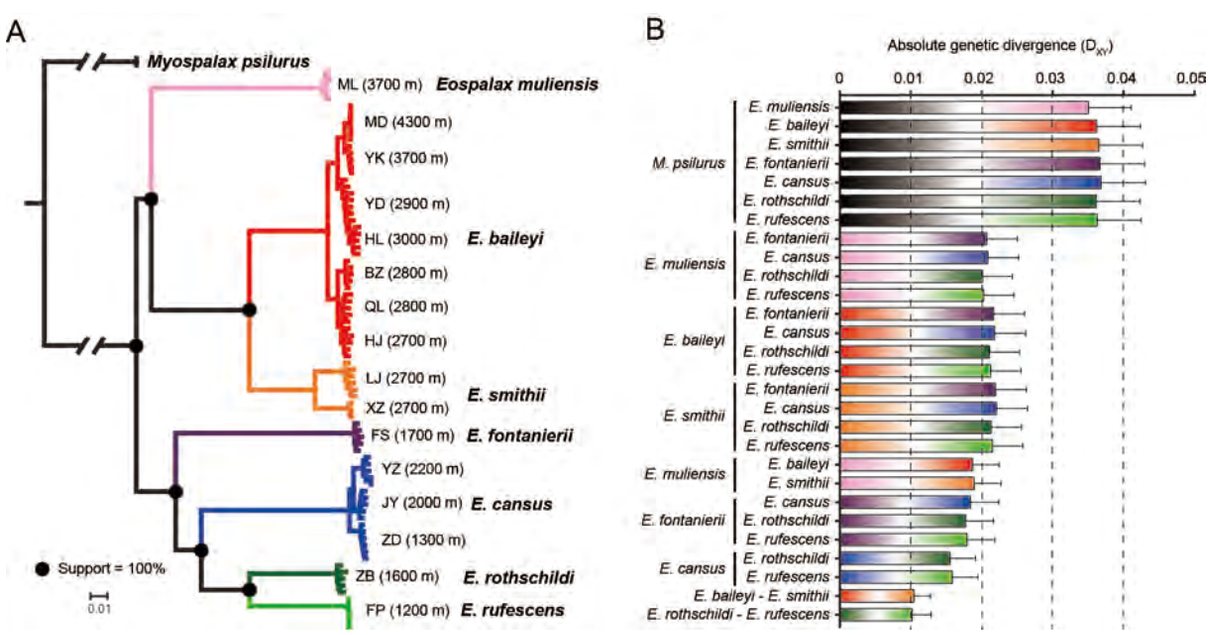

Figure 2 Phylogenetic relationships among species of *Eospalax*

A: ML phylogenetic tree from whole-genome SNVs; 100 bootstraps were applied; scale bar represents level of similarity. B: Pairwise genetic distance among species in genera *Myospalax* and *Eospalax*. Genetic distances were calculated in over 50 000 windows (50 kb in size) across whole genome. Data are mean±*SD*.

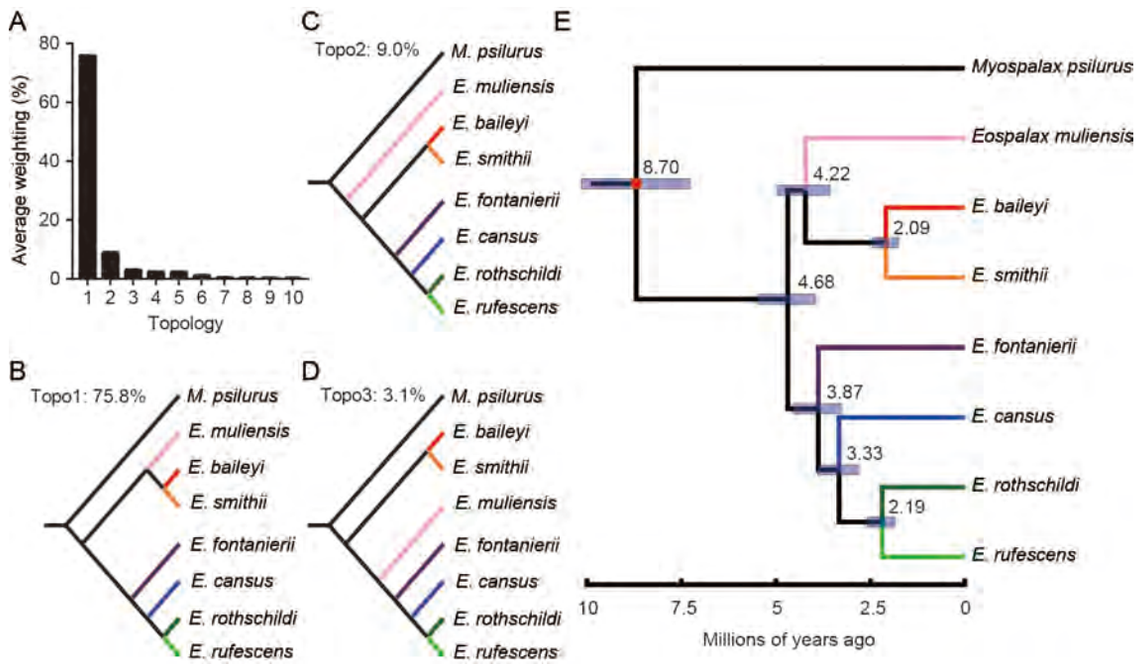

Figure 3 Alternative topologies and divergence times of genus *Eospalax*

Average weighting of ranked topologies in over 50 000 windows (50 kb in size) across whole genome (A). Three best topologies and their weighting are shown (B–D). Divergence times estimated using SNAPP based on whole-genome SNVs (E). Node numbers refer to divergence time, blue shadows represent 95% confidence intervals of divergent time. Red circle indicates node for split of *Myospalax* and *Eospalax* as a calibration point.

genome-based phylogenetic tree (Figure 3A, B). In addition, four alternative topologies were supported by at least 1% of windows (Figure 3A). The top two alternative topologies differed from the majority tree in the position of *Eospalax muliensis* **sp. nov**. (Figure 3C,D). The other two less-supported topologies revealed an uncertain relative position of *E. fontanierii* and *E. cansus* within the second clade (Supplementary Figure S2).

In divergence time analysis, all posterior trees sampled by SNAPP were identical to the whole-genome-based phylogenetic tree (Supplementary Figure S3). The two major high- and low-altitude clades diverged from each other ~4.68 Ma (95% CI=3.94–5.48 Ma) (Figure 3E). Shortly after, *Eospalax muliensis* **sp. nov**. diverged from *E. baileyi* and *E. smithii* (~4.22 Ma; 95% CI=3.57–4.97 Ma). Within the low-altitude clade, *E. fontanierii* first diverged from other species ~3.87 Ma (95% CI=3.26–4.54 Ma). Thus, the speciation events within the genus *Eospalax* generally occurred in the Pliocene (Figure 3E).

Morphometric comparison and morphological diagnosis

The external and craniodental measurements of each species are given in Table 2. A total of 57 intact skulls of adult specimens were used for PCA. The first three principal components (PC1–3) had eigenvalues greater than 1.0, and together accounted for >79.78% of total variance (Supplementary Table S2). PC1 accounted for 44.08% of the variation (eigenvalue=9.26) and was strongly loaded with most variables, except IOB, GBFM, DAB, and M^2–M^2, indicating it may be a marker of size. PC2 accounted for 21.57% of the variation (eigenvalue=4.53) and was strongly dominated by RSW, IOB, FIB, and LLI (loading>0.62), while PC3 accounted for 14.13% of the variation (eigenvalue=2.97) and was dominated by GBFM, DAB, and M^2–M^2.

The PC1–2 plot (Figure 4) showed that *Eospalax muliensis* **sp. nov**. occupied the lower-left corner and was well separated from the other species. Specimens of *Eospalax muliensis* **sp. nov**. were plotted on the negative field of both PC1 and PC2, reflecting its generally smaller size, narrower RSW, IOB, and FIB, and shorter LLI. Specimens of *E. baileyi* occupied a large area, from –1.34 to 1.45 in PC1 and –0.49 to 1.70 in PC2, indicating great variation in size, with a relatively wide RSW, IOB, and FIB, and long LLI. Specimens of *E. cansus*, *E. fontanierii*, *E. rufescens*, and *E. smithii* were mostly plotted on the positive region of PC1, indicating relatively large skulls.

Both molecular and morphological evidence supported *Eospalax muliensis* **sp. nov**. as a new species, which is formally described below.

Taxonomic account

***Eospalax muliensis* Zhang, Chen & Shi, sp. nov.**

Suggested common name: Muli zokor; 木里鼢鼠 (Muli Fenshu)

Holotype: KIZ 040324 (field No.: SC 2110385). Adult female collected by Tao Zhang, Meng-Long Lei, Zhong-Zheng Chen, and Hao Zhou on 21 April 2021. Dried skin, cleaned skull, and alcohol-preserved carcass are deposited in KIZ. Measurements (mm): BW=133.00 g, HB=172.0, TL=56.5, HF=28.0, GLS=39.41, CB=37.46, BL=35.40, PL=27.27, ZMW=25.58, IOB=7.27, FIB=6.12, RSW=8.84, MTW=22.95, M^2–M^2=9.30, LUTR=23.93, LUM=9.11, NSL=14.65, BCH=15.84, GBFM=6.25, LAB=8.33, DAB=4.12, MDL=24.75,

Table 2 Body weight and external and cranial measurements (mm) (mean±*SD* and ranges) of *Eospalax* specimens (*n*) examined in this study

Variable	*Eospalax muliensis*	*E. baileyi*	*E. cansus*	*E. fontanierii*	*E. rothschildi*	*E. rufescens*	*E. smithii*
	n=14	*n*=34	*n*=5	*n*=1	*n*=2	*n*=2*	*n*=4
BW	155.64±43.78 118.24–280.22; 12	248.44±73.20 133.63–384.33; 34	N/A	N/A	N/A	N/A	N/A
HB	168.92±14.64 145.00–204.00; 12	191.47±16.03 160.00–220.00; 34	N/A	N/A	N/A	N/A	N/A
TL	52.86±8.82 45.00–70.00; 7	N/A	N/A	N/A	N/A	N/A	N/A
HF	28.00±2.08 25.00–32.00; 7	N/A	N/A	N/A	N/A	N/A	N/A
GLS	40.52±1.83 38.01–45.52; 14	44.43±2.46 40.57–50.18; 32	44.38±3.07 41.45–49.05; 5	50.94	41.83±3.17 39.58–44.07; 2	40.60±4.10 37.70–43.50; 2	48.22±1.88 45.56–49.63; 4
CBL	38.15±1.90 35.55–43.34; 13	42.46±2.53 37.84–48.67; 32	42.17±3.32 39.33–47.09; 5	49.36	39.62±2.26 38.02–41.21; 2	37.82±4.38 34.72–40.91; 2	45.81±1.79 43.43–47.30; 4
BL	35.87±1.83 33.30–40.76; 13	40.14±2.59 35.55–46.44; 32	39.88±3.15 37.26–44.62; 5	46.29	37.58±2.31 35.95–39.21; 2	35.85±4.71 32.52–39.18; 2	43.20±1.86 40.78–44.86; 4
PL	27.02±1.21 25.60–30.39; 14	30.63±1.83 26.62–34.73; 32	30.74±2.32 28.72–34.18; 5	35.93	31.33±2.29 29.71–32.95; 2	26.84±2.49 25.08–28.60; 2	33.07±1.87 30.46–34.59; 4
ZMW	26.25±1.75 23.57–30.60; 14	30.83±2.91 25.75–36.58; 32	29.51±3.21 26.90–33.78; 5	37.01	29.06±3.73 26.42–31.70; 2	27.52±4.51 24.33–30.71; 2	34.76±2.93 30.47–36.88; 4
IOB	7.11±0.32 6.61–7.64; 14	7.80±0.37 6.95–8.37; 32	7.34±0.36 7.01–7.91; 5	8.53	7.81±0.33 7.57–8.04; 2	7.03±0.48 6.69–7.37; 2	8.04±0.27 7.69–8.33; 4
FIB	6.24±0.23 5.80–6.72; 14	8.67±0.76 7.32–10.28; 32	7.73±0.57 7.22–8.35; 5	8.62	7.60±1.03 6.87–8.33; 2	7.10±0.59 6.68–7.52; 2	9.07±0.79 8.04–9.75; 4
RSW	8.99±0.50 8.32–10.31; 14	11.54±0.77 10.22–13.31; 32	10.43±0.95 9.51–11.68; 5	13.84	10.10±1.19 9.26–10.94; 2	9.54±1.75 8.30–10.78; 2	12.26±0.97 11.13–13.23; 4
MTW	23.54±1.31 21.55–26.74; 14	27.70±2.25 23.44–31.77; 32	26.28±1.93 24.09–28.38; 5	35.60	26.11±3.39 23.71–28.50; 2	22.42±2.75 20.47–24.36; 2	29.99±2.31 26.59–31.69; 4
M^2–M^2	8.82±0.45 8.21–9.74; 14	9.02±0.44 8.37–10.33; 32	8.36±0.34 7.96–8.86; 5	10.21	8.68±0.52 8.31–9.04; 2	8.16±0.73 7.64–8.67; 2	9.24±0.62 8.42–9.88; 4
LUTR	23.94±1.28 22.33–27.45; 14	27.24±1.56 24.50–30.55; 32	27.19±2.12 24.97–29.96; 5	32.47	25.38±1.57 24.27–26.49; 2	24.29±3.00 22.17–26.41; 2	29.29±1.57 27.61–30.86; 4
LUM	8.95±0.46 8.33–10.26; 14	10.28±2.88 9.14–25.93; 32	10.34±0.65 9.70–11.19; 5	11.93	9.80±0.02 9.78–9.81; 2	9.34±1.02 8.62–10.06; 2	10.20±0.66 9.51–10.99; 4
NSL	14.55±1.17 12.41–17.37; 14	17.09±1.24 14.67–19.29; 32	16.40±1.08 15.17–17.98; 5	18.13	15.68±2.14 14.16–17.19; 2	15.60±2.14 14.08–17.11; 2	18.96±1.15 17.38–20.02; 4
BCH	16.20±0.66 15.35–17.80; 14	17.53±1.10 15.86–19.63; 32	16.87±1.51 15.69–18.99; 5	20.94	17.68±2.73 15.75–19.61; 2	14.47±0.78 13.91–15.02; 2	17.63±0.67 16.80–18.18; 4
GBFM	6.51±0.20 6.25–6.99; 13	6.63±0.28 6.04–7.05; 32	6.52±0.33 6.08–6.84; 5	6.96	6.25±0.18 6.12–6.37; 2	6.21±0.18 6.08–6.33; 2	6.58±0.52 5.91–7.19; 4
LAB	8.32±0.39 7.81–9.13; 14	9.27±0.57 8.44–11.08; 32	10.06±0.49 9.26–10.52; 5	11.09	9.19±0.81 8.61–9.76; 2	9.48±0.64 9.03–9.93; 2	10.48±0.25 10.14–10.75; 4
DAB	4.24±0.28 3.75–4.76; 14	4.93±0.89 4.01–9.21; 31	3.73±0.48 3.23–4.29; 5	5.77	3.75±0.29 3.54–3.95; 2	3.15±0.62 2.71–3.58; 2	4.91±0.76 3.88–5.72; 4
MDL	25.17±1.25 23.63–28.48; 14	26.95±1.50 23.71–29.86; 32	28.12±2.49 25.61–31.44; 5	33.40	26.28±1.75 25.04–27.51; 2	25.93±2.91 23.87–27.99; 2	28.59±1.53 27.01–30.08; 4
LBTR	19.65±1.27 18.05–22.68; 14	22.12±1.43 18.55–25.18; 32	21.67±1.43 20.11–23.33; 5	26.23	20.14±2.05 18.69–21.59; 2	19.93±2.86 17.90–21.95; 2	25.15±1.05 24.17–26.25; 4
LLM	9.43±0.46 8.81–10.34; 14	10.02±0.35 9.29–10.57; 32	10.39±0.61 9.68–11.23; 5	12.39	10.05±0.06 10.00–10.09; 2	10.25±1.16 9.43–11.07; 2	10.73±0.59 9.96–11.39; 4
LLI	8.59±1.51 6.40–10.84; 14	11.61±2.00 7.97–15.95; 32	10.11±1.72 7.80–12.05; 5	13.53	8.82±2.65 6.94–10.69; 2	10.22±2.79 8.24–12.19; 2	15.63±0.86 14.83–16.53; 4

Character abbreviations (unless specifically, all in mm): BW: Body weight (grams); HB: Head and body length; TL: Tail length; HF: Hindfoot length; GLS: Greatest length of skull; CBL: Condylobasal length; BL: Basal length; PL: Palatal length; ZMW: Zygomatic width; IOB: Interorbital breadth; FIB: Foramen infraorbital breadth; RSW: Rostrum width; MTW: Mastoid width; M^2–M^2: Maximum width across the upper second molars; LUTR: Length of upper tooth row; LUM: Length of upper molars; NSL: Nasal length; BCH: Braincase height; GBFM: Greatest breadth of the foramen magnum; LAB: Length of auditory bulla; DAB: Distance between auditory bulla; MDL: Mandibular length; LBTR: Length of below toothrow; LLM: Length of lower molars; LLI: Length of lower incisor. *: The smaller value is from a subadult individual. N/A: Not available.

LBTR=20.36, LLM=9.63, LLI=10.51.

Type locality: Kangwu Ranch (N28.135°, E101.196°), Muli County, Sichuan Province, China, adjacent to Shangri-La Lake at an altitude of ~3 700 m a.s.l.

Paratypes: Seven specimens were collected from the type locality. Four specimens (KIZ 040325–040328) were deposited in KIZ, CAS; three specimens (SC 2110384, 2110386, and 2110451) were deposited in the Biological Museum of Anhui Normal University. All specimens were prepared as dried skins with cleaned skulls and alcohol-preserved carcasses.

Etymology: The species name *muliensis* is derived from Muli

County, the type locality of the new species in Sichuan Province, China, and the Latin adjectival suffix *-ensis* means “belonging to”.

Diagnosis: *Eospalax muliensis* **sp. nov.** can be distinguished from other described species of *Eospalax* by a combination of the following characters: size small (mean BW=155.64 g; mean GLS=40.52 mm); tail relatively long, densely hairy; nose-pad trifoliate; rostrum weak, nearly rectangular, nasals small, posterior border of nasals transverse, anterior halves of premaxilla nearly aligned with nasals; braincase well-domed, temporal ridges not conspicuous, parallel in front, lambdoid crests only present on side of skull; occipital shield with developed occipital ridges, extending well posteriorly, almost forming plane with occipital condyle; about 1/3 of incisive foramina included within maxillae, remaining 2/3 of incisive foramina included within premaxillae; palate and pterygopalatine fossa large, M^2–M^2 almost equal to LUM; M^3 with two reentrant angles on outer side.

Description: Small-sized zokor (Table 2), with head and body length <175 mm (range: 145.0–175.0 mm) and skull length <42.20 mm (range: 38.01–42.17 mm). Only one elderly male (KIZ 0403327) significantly larger, with head and body length of 204 mm and skull length of 45.52 mm. Dorsal pelage dark grayish brown, with slightly cinnamon-colored tips, ventral pelage slightly paler; most individuals without white blaze on forehead, small when present. Lips and muzzle white, surrounded by short white hairs. Nose-pad trifoliate. Eyes very small and external ears absent (Figure 1B). Tail relatively long, densely hairy, proximal 2/3 grayish-brown, and distal 1/3 white. Forepaws strong and powerful; third claw longest and stoutest; second and fourth claws almost equal in length, about 2/3 of third claw; fifth claw stout, about half length of fourth finger; thumb very small. Dorsal surfaces of hands and feet covered with short white hair.

Skull relatively weaker than other zokors (Figure 5). Rostrum relatively weak, thin, and nearly rectangular; nasals relatively small and trapezoidal, extending far beyond incisors, posterior border of nasals transverse. Premaxilla

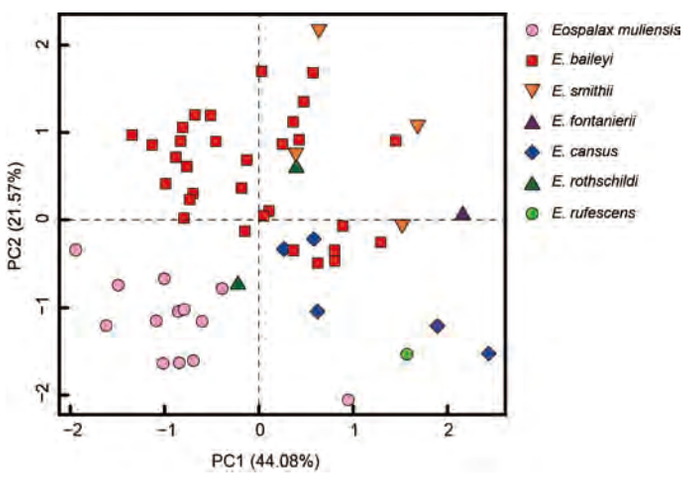

Figure 4 Plot of principal components 1 and 2 from analysis of 21 craniodental measurements of *Eospalax* genus

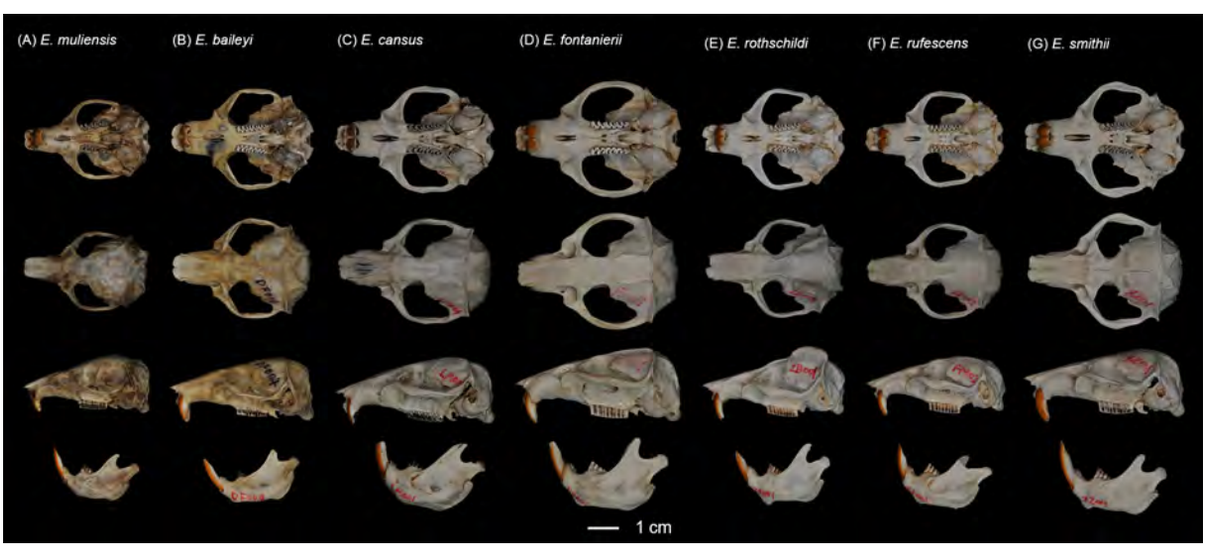

Figure 5 Dorsal, ventral, and lateral views of skull and mandible of *Eospalax muliensis* sp. nov. (KIZ 040324, holotype) (A), *E. baileyi* (DF 004) (B), *E. cansus* (LM 001) (C), *E. fontanierii* (FS 001) (D), *E. rothschildi* (ZB 001) (E), *E. rufescens* (FP 001) (F), and *E. smithii* (XZ 001) (G)

undeveloped, anterior half not expanded, nearly aligned with nasals. Zygomatic arches slightly expanded and thin; zygomatic plates narrow and simple. Interorbital region slightly constricted, almost same width as rostrum. Braincase well-domed, rounded ventrally. Temporal ridges not conspicuous (but much more developed in old male KIZ 0403327), parallel in front. Lambdoid crests sharp, but only on side of skull; occipital shield and occipital ridges developed, extending well posteriorly, almost forming plane with occipital condyle; small medial occipital ridge present between occipital ridges. Incisive foramina small, about 2/3 included within premaxilla, posterior 1/3 within maxillaries. Palate and pterygopalatine fossa broad, relatively wider than other *Eospalax* species. Body of mandible curved. Coronoid process weak, pointed, and curved to posterior. Condyloid process stout and squared. Angular process small, curved upward almost joining with ramus.

Teeth relatively light. Incisor teeth stout with tips curving slightly backward, outer side orange. Upper molar tooth rows slightly divergent to posterior; M^1 with two reentrant angles on outer and inner side; M^2 and M^3 with two reentrant angles on outer side, and one inside, no postero-external lobe on M^3; lower incisor short, slightly curved, outer side orange; M_1 with two reentrant angles on outer side and three on inner side; M_2 and M_3 with two reentrant angles on outer and inner sides.

Comparison: According to the measurements, *Eospalax muliensis* **sp. nov**. is similar in size to *E. rothschildi*, but much smaller than other species in all dimensions (Table 2; Supplementary Table S3). The new species has some features unique in the genus. The skull of *Eospalax muliensis* **sp. nov.** is obviously weaker than that of the other *Eospalax* species, especially in the rostrum region (Figure 5). Therefore, the rostrum-related measurements (i.e., RSW, FIB, and NSL) of *Eospalax muliensis* **sp. nov**. are the smallest among *Eospalax* species (Table 2). The nasals of the new species are very short and narrow, the smallest in the genus. The premaxilla of *Eospalax muliensis* **sp. nov.** is depressed and very thin, with the anterior half parts nearly aligned with the nasals, in contrast with other species, in which the premaxillae are well-developed and broader than the nasals. The palate and pterygopalatine fossa are relatively wider in *Eospalax muliensis* **sp. nov** than in other species, thus M^2–M^2 is almost equal to LUM in the new species but is much smaller than LUM in other species. The braincase of *Eospalax muliensis* **sp. nov.** are well-domed and temporal ridges being ambiguous, characteristics only seen in some individuals of *E. cansus* and different from the flattened braincase with developed temporal ridges seen in other species.

Eospalax muliensis **sp. nov.** can be distinguished from small-sized *E. rothschildi* by its strong and powerful forepaws (vs. slender); longer tail TL=45–70 mm (vs. short tail TL=23–38 mm, Supplementary Table S3); and proximal 2/3 of tail grayish-brown and distal 1/3 white (vs. gray above white below). *Eospalax muliensis* **sp. nov.** can be distinguished from *E. fontanierii* and *E. cansus* based on trifoliate nose-pad and densely hairy tail (vs. oval nose-pad and nearly naked tail). *Eospalax muliensis* **sp. nov.** can be clearly distinguished from *E. baileyi* and *E. smithii* based on incisive foramina about 1/3 expanding premaxillary boundaries (vs. incisive foramina wholly contained in premaxillary). *Eospalax muliensis* **sp. nov.** can be distinguished from *E. baileyi* by the postero-external lobe on M^3; the parallel temporal ridges of *E. muliensis* **sp. nov.** is distinct from the temporal ridges meeting in the median line of *E. smithii*. The zygomatic arches of *E. rufescens* are much stouter and flare wider than *Eospalax muliensis* **sp. nov**.

Distribution and habitat: *Eospalax muliensis* **sp. nov.** is currently known only from the Kangwu Ranch, Muli County, Sichuan Province, China (elevational range ~3 700 m a.s.l.). The habitat is alpine meadow, surrounded by shrubs (Supplementary Figure S4). This species may be adapted to high-elevation habitats, and thus may occur in other alpine meadows in the southern Hengduan Mountains.

DISCUSSION

Taxonomic implications

Both morphological and molecular analyses strongly suggested that the zokors inhabiting Muli County represent a new species (*Eospalax muliensis* **sp. nov.**) of *Eospalax*. The new species can be diagnosed from all others within *Eospalax* by the combination of small size, long tail, weak rostrum and nasal, and large palate and pterygopalatine fossa. Genomic analyses also revealed that *Eospalax muliensis* **sp. nov.** diverged from other recognized zokor species ~4.22 Ma, with high genetic distances in nuclear and mitochondrial genomes.

Our results also strongly supported the status of all six previously described *Eospalax* species. The most recent divergences in *Eospalax* occurred between *E. baileyi* and *E. smithii*, and between *E. rufescens* and *E. rothschildi*. Evidence revealed substantial differences among the two pairs of sister species and supported their species status. First, based on whole-genome analysis, the two species pairs diverged 2.09 Ma and 2.19 Ma (Figure 3E), with relatively high genetic distances of 1.05% and 1.02% (Figure 2B), respectively. Genetic distances of the mitochondrial cyt *b* gene between sister species of these pairs reached 11.9% and 12.5%, respectively (Supplementary Table S4) (Bradley & Baker, 2001). Second, the morphological characteristics that distinguish these sister species have been long recognized. For example, *E. smithii* can be distinguished from *E. baileyi* based on temporal ridges meeting at the median line (Figure 5) (Fan & Shi, 1982); and *E. rothschildi* can be distinguished from *E. rufescens* based on temporal ridges conspicuous and raised (Figure 5) (Fan & Shi, 1982). Third, the distribution of habitats differs among these sister species. *Eospalax baileyi* is dominant on the QTP (altitudinal range of 2 700–4 300 m a.s.l.), while *E. smithii* inhabits a small area around the Min Mountains (eastern edge of QTP) at an altitude of 2 700 m a.s.l. and possibly around the Liupanshan Mountains (within the Loess Plateau) at much lower altitudes (Fan & Shi, 1982). In the second sister species pair, *E. rufescens* occurs in the Qinling Mountains, while *E. rothschildi* occurs in the Daba Mountains and probably the Min Mountains. Although the forest habitats of these two species are similar, their local climate and flora differ, and they are likely geographically isolated by the Hanjiang River. In summary, genomic, morphological, and biogeographical

evidence well supports the delimitation of these two pairs of recently diverged sister species. Furthermore, the status of other species within *Eospalax* that were divergent longer before should also be retained.

Phylogenetic implications

Utilizing whole-genome sequencing data, our study revealed reliable and robust phylogenetic relationships among species in the genus *Eospalax*. Before discussing the implications of the whole-genome-based phylogenetic relationships, we first explored the significant incongruences among phylogenies inferred from nuclear genomes, mitogenomes, and previous studies. Regarding phylogenies inferred from mitogenomes and mitochondrial genes, our results and previous studies show general similarity in the close relationship between *E. baileyi* and *E. smithii* and the basal position of *E. fontanierii* (Supplementary Figure S1) (Cai et al., 2020; He et al., 2012, 2020; Su et al., 2014). However, extensive inconsistencies appear in mitochondrial analyses, which may be due to the limited informative sites of mitochondrial genes and complex speciation and post-speciation processes in the genus *Eospalax*. For the latter, some clues may be present in our mitogenomic analysis that integrates the mitogenomes in our and previously published data. Our mitogenomic analyses revealed a robust phylogeny but embedded one *E. cansus* (KC514112) individual tightly within *E. baileyi* (Supplementary Figure S1). This individual was reportedly sampled from Lintan County, Gansu Province (around Min Mountains) (Su et al., 2013), which contains the type localities of *E. cansus*, *E. rothschildi*, and *E. smithii*. Furthermore, *E. baileyi* habitats are also adjacent to this region. Besides the possible misidentification of the specimen or habitat expansion of *E. baileyi* in Lintan, another plausible explanation may be post-speciation gene flow between *E. cansus* and *E. baileyi* around the Min Mountains. If this hypothesis is true, the evolutionary history of zokors around the Min Mountains may be more complex, which requires further research.

Several incongruences in the phylogenetic topologies inferred from nuclear and mitochondrial genomes were also found. Notably, nuclear genomic analysis placed *E. fontanierii* within the low-altitude clade (Figure 2A), whereas mitogenomic analysis and most previous studies placed *E. fontanierii* in a basal position, while *Eospalax muliensis* **sp. nov.** were put aside (Supplementary Figure S1). In addition, nuclear genomic analysis placed *Eospalax muliensis* **sp. nov.** within the high-altitude clade (Figure 2A), while mitogenomic analysis placed it in the basal position of the genus (Supplementary Figure S1). Nuclear and mitochondrial discordance appears to be prevalent in phylogenetic studies and the possible roles of rapid speciation and incomplete lineage sorting have been discussed extensively (He et al., 2010; Mckay & Zink, 2010). Rapid speciation and incomplete lineage sorting may have contributed to the inconsistent relationships found among *E. cansus*, *E. rufescens*, and *E. rothschildi*, given the rapid cladogenesis of these three species (Figures 2A, 3E). Other factors may also have contributed to the inconsistent positions of *E. fontanierii* and *Eospalax muliensis* **sp. nov**. For example, the clear pattern of mitochondrial phylogenomic analyses is the relevance between geographical distributions and phylogenetic positions of the species in *Eospalax*. *Eospalax fontanierii* and *Eospalax muliensis* **sp. nov.** are distributed in the remote northeast and southwest regions (Figure 1A), and their phylogenetic positions are basal. Furthermore, other species are geographically and phylogenetically adjacent. The possible explanation for this pattern may be ancient cross-species hybridization between geographically adjacent species or some other geographically relevant factors (Toews & Brelsford, 2012). However, these hypotheses lack solid evidence and require further comprehensive investigations. Regardless of the actual source of incongruence, the phylogeny inferred from nuclear genomes was more robust and thus serves as our current "best" estimate (Figure 2A).

From the inferred nuclear whole-genome-based phylogeny, *Eospalax* was first divided into high- and low-altitude clades. Because uplift of the QTP may predate the separation of these two clades (Spicer et al., 2021) and no other species in the subfamily Myospalacinae or family Spalacidae inhabit the QTP, adaptation to high altitude may have occurred in the common ancestor of *Eospalax muliensis* **sp. nov.**, *E. baileyi*, and *E. smithii*. Nowadays, *E. smithii* inhabits areas at relatively low altitudes, implying possible re-adaptation to low elevations. Notably, given the possible existence of other unrecognized species in the Hengduan Mountains, adaptation to high altitude could have occurred in the common ancestor of all *Eospalax* species. Within the low-altitude clade, successful habitation of forest niches appeared in *E. rufescens* and *E. rothschildi*. Because these two species are closely related and separated more recently (Figures 2A, 3E), forest adaptation likely occurred in their common ancestor. Thus, although the dispersal capacity of zokors is extremely limited (Wei et al., 1997), species in *Eospalax* successfully and rapidly adapted to diverse ecological niches in the Pliocene, and further investigations on their adaptive mechanisms are warranted.

Implications of systematics and macroevolution from Muli zokors

The discovery of *Eospalax muliensis* **sp. nov.** in the southern Hengduan Mountains is unexpected and of great interest because the habitats of *Eospalax muliensis* **sp. nov.** are southernmost of extant zokors and it is the second extant zokor species that inhabit extremely high altitudes (~3 700 m a.s.l.). The Hengduan Mountains are considered a global biodiversity hot spot (Myers et al., 2000). The extremely diverse ecological habitats in three dimensions of Hengduan Mountains (Sky islands) protected species from climate fluctuations and are known inhabited by some relict species (Chen et al., 2017; Chen et al., 2021; He & Jiang, 2014). The discovery of *Eospalax muliensis* **sp. nov.** in such a biodiverse area suggests the possible existence of other unknown zokor species in the Hengduan Mountains. On the other hand, the discovery could also provide clues for deciphering the origin and evolutionary history of the genus *Eospalax*.

Based on the paleontological rules and evolutionary trajectories of zokor fossils, Li & Chen (1986) proposed nine plesiomorphic characters of ancient *Eospalax* species. Strikingly, of the nine characters, six are found in *Eospalax*

muliensis **sp. nov.**, in contrast to the five or fewer in other species in *Eospalax*. For example, body size trajectory in zokor fossils is from small- to large-sized (Zheng, 1994), whereas *Eospalax muliensis* **sp. nov.** is among the smaller ones in *Eospalax*. *Eospalax muliensis* **sp. nov.** also possesses other plesiomorphic characters such as: long tail; weak rostrum and nasal; slightly expanded and thin zygomatic arch; ambiguous temporal ridge; and separated temporal ridge. Absent of *Eospalax muliensis* **sp. nov.**, previous studies proposed the Loess Plateau or Qinling-Daba Mountains as the possible origin center of *Eospalax* (Li & Chen, 1986; Li & Wang, 1996). Considering the plesiomorphic characters and relatively basal phylogenetic position of *Eospalax muliensis* **sp. nov.**, it is possible that *Eospalax* may have originated from the Hengduan Mountains. This hypothesis seems to contradict fossil evidence, as the earliest known *Eospalax* fossils are recorded from the Nihewan Basin, Hebei Province (Zheng, 1994) and are dated to ~2 Ma (MN18) (Li et al., 1984). However, the estimated diversification of *Eospalax* species occurred ~4.68 Ma, and thus the contradiction may be caused by an incomplete *Eospalax* fossil record, especially in the Hengduan Mountains. Therefore, the origin and evolutionary history of *Eospalax* remain obscure and require further interdisciplinary evidence.

SCIENTIFIC FIELD SURVEY PERMISSION INFORMATION

All collections followed the animal use protocols approved by the Animal Care and Ethics Committee of the Kunming Institute of Zoology, Chinese Academy of Sciences (Approval No. SMKX-SQ-2021-067). Permission for field sampling in each sampling sites was granted by the local Forestry Bureau.

DATA AVAILABILITY

All sequences reported in this study were deposited in the Genome Sequence Archive database (http://gsa.big.ac.cn/) under Accession ID (CRA005933) and in Science Data Bank (https://www.scidb.cn/) under DOI: 10.11922/sciencedb.o00023.00002. Mitogenomes were deposited in GenBank under Accession Nos. OM329951–OM330035.

SUPPLEMENTARY DATA

Supplementary data to this article can be found online.

COMPETING INTERESTS

The authors declare that they have no competing interests.

AUTHORS' CONTRIBUTIONS

P.S. conceived and supervised the study. T.Z., M.L.L., H.Z., and Z.Z.C. collected samples. Z.Z.C. and T.Z. performed morphometric comparison and morphological diagnosis. T.Z. analyzed whole-genome resequencing data. T.Z., Z.Z.C., and P.S. wrote the paper. All authors read and approved the final version of the manuscript.

ACKNOWLEDGMENTS

We are grateful to Bao-Guo Li (Northwest University) for sharing sample sites and helpful discussion. We are grateful to Jia-Tang Li (Chengdu Institute of Biology, Chinese Academy of Sciences), Zheng-Jun He (Animal Husbandry Bureau of Tibetan Autonomous County of Muli, Sichuan Province), and Shi-Yan Ding (Forestry Bureau of Zhenba County, Shaanxi Province) for help in field sampling.

REFERENCES

Allen GM. 1940. The Mammals of China and Mongolia, Part 2. New York: The American Museum of Natural History.

Bolger AM, Lohse M, Usadel B. 2014. Trimmomatic: a flexible trimmer for Illumina sequence data. *Bioinformatics*, **30**(15): 2114−2120.

Bouckaert R, Vaughan TG, Barido-Sottani J, Duchêne S, Fourment M, Gavryushkina A, et al. 2019. BEAST 2.5: an advanced software platform for Bayesian evolutionary analysis. *PLoS Computational Biology*, **15**(4): e1006650.

Bradley RD, Baker RJ. 2001. A test of the genetic species concept: cytochrome-*b* sequences and mammals. *Journal of Mammalogy*, **82**(4): 960−973.

Bryant D, Bouckaert R, Felsenstein J, Rosenberg NA, Roychoudhury A. 2012. Inferring species trees directly from biallelic genetic markers: bypassing gene trees in a full coalescent analysis. *Molecular Biology and Evolution*, **29**(8): 1917−1932.

Cai ZY, Zhang JJ, Qiao PH, Qing W, Zhang TZ. 2020. Next generation sequencing yields the complete mitogenome of Smith's zokor (*Eospalax smithii*). *Mitochondrial DNA Part B*, **5**(3): 2109−2110.

Chen ZZ, He K, Huang C, Wan T, Lin LK, Liu SY, et al. 2017. Integrative systematic analyses of the genus *Chodsigoa* (Mammalia: Eulipotyphla: Soricidae), with descriptions of new species. *Zoological Journal of the Linnean Society*, **180**(3): 694−713.

Chen ZZ, He SW, Hu WH, Song WY, Onditi KO, Li XY, et al. 2021. Morphology and phylogeny of scalopine moles (Eulipotyphla: Talpidae: Scalopini) from the eastern Himalayas, with descriptions of a new genus and species. *Zoological Journal of the Linnean Society*, **193**(2): 432−444.

Danecek P, Auton A, Abecasis G, Albers CA, Banks E, Depristo MA, et al. 2011. The variant call format and VCFtools. *Bioinformatics*, **27**(15): 2156−2158.

Fan NC, Shi YZ. 1982. A revision of the zokors of subgenus *Eospalax*. *Acta Theriologica Sinica*, **2**(2): 183–199. (in Chinese)

Guo YT, Zhang J, Xu DM, Tang LZ, Liu Z. 2021. Phylogenomic relationships and molecular convergences to subterranean life in rodent family Spalacidae. *Zoological Research*, **42**(5): 671−674.

He K, Jiang XL. 2014. Sky islands of Southwest China. I: an overview of phylogeographic patterns. *Chinese Science Bulletin*, **59**(7): 585−597.

He K, Li YJ, Brandley MC, Lin LK, Wang YX, Zhang YP, et al. 2010. A multi-locus phylogeny of Nectogalini shrews and influences of the paleoclimate on speciation and evolution. *Molecular Phylogenetics and Evolution*, **56**(2): 734−746.

He Y, Hu SZ, Ge DY, Yang QS, Connor T, Zhou CQ. 2020. Evolutionary history of Spalacidae inferred from fossil occurrences and molecular phylogeny. *Mammal Review*, **50**(1): 11−24.

He Y, Zhou CQ, Liu GK, Chen L, Zhang Y, Pan L. 2012. Research on the validity of *Eospalax smithi* inferred from molecular and morphological evidences. *Acta Zootaxonomica Sinica*, **37**(1): 36−43. (in Chinese)

Jiang ZG, Liu SY, Wu Y, Jiang XL, Zhou KY. 2017. China's mammal diversity (2nd edition). *Biodiversity Science*, **25**(8): 886−895. (in Chinese)

Jin JJ, Yu WB, Yang JB, Song Y, Depamphilis CW, Yi TS, et al. 2020.

GetOrganelle: a fast and versatile toolkit for accurate de novo assembly of organelle genomes. *Genome Biology*, **21**(1): 241.

Lanfear R, Frandsen PB, Wright AM, Senfeld T, Calcott B. 2017. PartitionFinder 2: new methods for selecting partitioned models of evolution for molecular and morphological phylogenetic analyses. *Molecular Biology and Evolution*, **34**(3): 772−773.

Larkin MA, Blackshields G, Brown NP, Chenna R, McGettigan PA, McWilliam H, et al. 2007. Clustal W and clustal X version 2.0. *Bioinformatics*, **23**(21): 2947−2948.

Li BG, Chen FG. 1986. Studies on the phylogenetic relationship, the speciation and the place of the origin of the subgenus *Eospalax*, *Genus Myospalax*. *Journal of Northwest University*, **16**(3): 59–66. (in Chinese)

Li BG, Chen FG. 1989. A taxonomic study and new subspecies of the subgenus *Eospalax*, genus *Myospalax*. *Acta Zoologica Sinica*, **35**(1): 89–95. (in Chinese)

Li CK, Wu WY, Qiu ZD. 1984. Chinese neogene: subdivision and correlation. *Vertebrata Palasiatica*, **22**(3): 163−178. (in Chinese)

Li H. 2012. Exploring single-sample SNP and INDEL calling with whole-genome *de novo* assembly. *Bioinformatics*, **28**(14): 1838−1844.

Li H. 2015a. BFC: correcting Illumina sequencing errors. *Bioinformatics*, **31**(17): 2885−2887.

Li H. 2015b. FermiKit: assembly-based variant calling for Illumina resequencing data. *Bioinformatics*, **31**(22): 3694−3696.

Li H. 2018. Minimap2: pairwise alignment for nucleotide sequences. *Bioinformatics*, **34**(18): 3094−3100.

Li XC, Wang TZ. 1996. Taxonomy and phylogeny of subgenus *Eospalax*. *Journal of Shaanxi Normal University*: *Natural Science Edition*, **24**(3): 75–78. (in Chinese)

Li YW, Lu JQ, Wang ZL. 2016. Complete mitochondrial genome of Manchurian Zokor (*Myospalax psilurus*). *Mitochondrial DNA Part A*, **27**(2): 1461−1462.

Lin GH, Wang K, Deng XG, Nevo E, Zhao F, Su JP, et al. 2014. Transcriptome sequencing and phylogenomic resolution within Spalacidae (Rodentia). *BMC Genomics*, **15**: 32.

Liu Y, Zhang ZR, He ZJ, He SP. 2007. Dynamic monitoring of rodents damage in damage-free demonstration grassland in Liangshan Yi Autonomous Prefecture. *Journal of Grassland and Forage Science*, (7): 44−46. (in Chinese)

Luo ZX, Chen W, Gao W. 2000. Fauna Sinica: Cricetidae. Beijing: Science Press, 148–178. (in Chinese)

Martin SH, van Belleghem SM. 2017. Exploring evolutionary relationships across the genome using topology weighting. *Genetics*, **206**(1): 429−438.

McKay BD, Zink RM. 2010. The causes of mitochondrial DNA gene tree paraphyly in birds. *Molecular Phylogenetics and Evolution*, **54**(2): 647−650.

Meng GL, Li YY, Yang CT, Liu SL. 2019. MitoZ: a toolkit for animal mitochondrial genome assembly, annotation and visualization. *Nucleic Acids Research*, **47**(11): e63.

Myers N, Mittermeier RA, Mittermeier CG, Da Fonseca GAB, Kent J. 2000. Biodiversity hotspots for conservation priorities. *Nature*, **403**(6772): 853−858.

Norris RW, Zhou KY, Zhou CQ, Yang G, William Kilpatrick C, Honeycutt RL. 2004. The phylogenetic position of the zokors (Myospalacinae) and comments on the families of muroids (Rodentia). *Molecular Phylogenetics and Evolution*, **31**(3): 972−978.

Pan QH, Wang YX, Yan K. 2007. A Field Guide to the Mammals of China. Beijing: China Forestry Publishing House. (in Chinese)

Rambaut A, Drummond AJ, Xie D, Baele G, Suchard MA. 2018. Posterior summarization in Bayesian phylogenetics using Tracer 1.7. *Systematic Biology*, **67**(5): 901−904.

Smith AT, Xie Y. 2008. A Guide to the Mammals of China. Princeton: Princeton University Press.

Song SY. 1986. A revision of the two species of the zokors on subgenus *Eospalax*. *La Animals Mondo*, **3**(3): 31–39.

Spicer RA, Su T, Valdes PJ, Farnsworth A, Wu FX, Shi GL, et al. 2021. Why 'the uplift of the Tibetan Plateau' is a myth. *National Science Review*, **8**(1): nwaa091.

Stamatakis A. 2014. RAxML version 8: a tool for phylogenetic analysis and post-analysis of large phylogenies. *Bioinformatics*, **30**(9): 1312−1313.

Su JH, Ji WH, Wang J, Gleeson DM, Zhou JW, Hua LM, et al. 2014. Phylogenetic relationships of extant zokors (Myospalacinae) (Rodentia, Spalacidae) inferred from mitochondrial DNA sequences. *Mitochondrial DNA*, **25**(2): 135−141.

Su JH, Wang J, Hua LM, Gleeson D, Ji WH. 2013. Complete mitochondrial genome of the Gansu zokor, *Eospalax cansus* (Rodentia, Spalacidae). *Mitochondrial DNA*, **24**(6): 651−653.

Toews DPL, Brelsford A. 2012. The biogeography of mitochondrial and nuclear discordance in animals. *Molecular Ecology*, **21**(16): 3907−3930.

Wei DB, Wei L, Zhang JM, Yu HY. 2006. Blood-gas properties of plateau zokor (*Myospalax baileyi*). *Comparative Biochemistry and Physiology Part A:Molecular & Integrative Physiology*, **145**(3): 372−375.

Wei FW, Yang QS, Wu Y, Jiang XL, Liu SY, Li BG, et al. 2021. Catalogue of mammals in China (2021). *Acta Theriologica Sinica*, **41**(5): 487−501. (in Chinese)

Wei WH, Wang QY, Zhou WY, Fan NC. 1997. The population dynamics and dispersal of plateau zokor after removing. *Acta Theriologica Sinica*, **17**(1): 53−61. (in Chinese)

Wilson DE, Reeder DM. 2005. Mammal Species of the World: A Taxonomic and Geographic Reference. 3rd ed. Baltimore: Johns Hopkins University Press.

Xu DM, Yang CP, Shen QS, Pan SK, Liu Z, Zhang TZ, et al. 2021. A single mutation underlying phenotypic convergence for hypoxia adaptation on the Qinghai-Tibetan Plateau. *Cell Research*, **31**(9): 1032−1035.

Zhang T, Chen J, Zhang J, Guo YT, Zhou X, Li MW, et al. 2021. Phenotypic and genomic adaptations to the extremely high elevation in plateau zokor (*Myospalax baileyi*). *Molecular Ecology*, **30**(22): 5765−5779.

Zheng SH. 1994. Classification and evolution of the Siphneidae. *In*: Tomida Y, Li CK, Setoguchi T. Rodent and Lagomorph Families of Asian Origins and Diversification. Tokyo: National Science Museum Monographs, 57–76.

Zhou CQ, Zhou KY. 2008. The validity of different zokor species and the genus *Eospalax* inferred from mitochondrial gene sequences. *Integrative Zoology*, **3**(4): 290−298.

Zou Y, Xu M, Ren SE, Liang NN, Han CX, Nan XN, et al. 2020. Taxonomy and phylogenetic relationship of zokors. *Journal of Genetics*, **99**(1): 38.